A two-dimensional multilevel adaptive finite element method for the time-independent Schrödinger equation

J. Ackermann and R. Roitzsch
Konrad-Zuse-Zentrum Berlin (ZIB), Heilbronner Strasse 10, D-10711 Berlin, Germany

Received 18 May 1993; in final form 16 August 1993

The subject of this study is a multilevel 2D finite element method (FEM) based on a local error estimator and self-adaptive grid refinement as a universal tool for solving stationary Schrödinger eigenvalue problems. Numerical results for standard problems appearing in vibrational motion and molecular electronic structure calculations are given and discussed. Results of relative precision 10^{-8} are obtained. For the linear H_3^{2+} system the adaptive FEM turns out to be superior to global basis set expansions in the literature.

1. Introduction

An alternative approach to algebraic approximations in molecular structure calculations can be seen in fully numerical methods, like the finite difference method (FDM) or the finite element method (FEM). The treatment of H_2^+ without the Born–Oppenheimer approximation [1], the solution of the Hartree–Fock–Slater equations [2], or the relativistic Dirac equation [3], as well as reactive scattering studies [4], are examples from a broad field where the FEM supports theoretical progress. But despite their success, up to now the FEM is not a standard method for quantum-chemical calculations. In most cases careful selection of special coordinates (appropriate to the shape of the eigenfunction) and point distribution is necessary to get accurate results. In the past, the applicability of this method to molecular systems without special symmetry properties was doubted for this reason [5]. A method is still lacking in which the grid is adapted automatically to the problem, avoiding the necessity of special coordinate systems and restriction to two-center problems.

We are studying a FEM based on an error estimator and multilevel adaptive grid refinement as a method for solving Schrödinger eigenvalue problems. The concept of adaptive refined grids is well known in numerical methods in engineering [6,7], but has never been applied to quantum-chemical eigenvalue problems. We use the adaptive program KASKADE [8], originally written for elliptic boundary value problems, and add modules (Givens method, inverse vector iteration, higher-order shape functions, high-order Gaussian integration) for application to eigenvalue problems. The precision of the adaptive FEM with linear elements turns out to be of the order of 10^{-3}, which is sufficient for most engineering applications. Higher-precision eigenvalues (in the range 10^{-6}–10^{-8}) become reachable by using higher-order polynomial shape functions ($p=1$, 2, 3). The program can be used for any form of the kinetic energy and the potential. It turns out that the choice of special coordinates is not necessary to achieve high-precision variational energy values. Thus, for molecular electronic structure calculation the adaptive FEM is not, as is the standard FEM, restricted to two-center problems. For the linear three-center one-electron system (linear H_3^{2+}) the adaptive FEM is superior to global basis set expansions in the literature.

In section 2, the proposed method is summarized briefly. In section 3, we give numerical results for different problems; more precisely, the six smallest eigenvalues of the non-isotropic two-dimensional harmonic oscillator, the ground state energies of the molecule ion H_2^+ at $R=2.0$, and the linear H_3^{2+} system at $R_1=R_2=1.0$, respectively, serve as examples

to test this method. The results are compared with exact results (as available) and other treatments in the literature. Also, inferences concerning the convergence behaviour and the variational principle are discussed. A short summary and outlook is given in section 4.

2. Outline of the method

For a variational treatment of the 2D Schrödinger equation

$$(\hat{H}-\lambda)\Psi=0 \tag{1}$$

we have to handle two problems:

(a) We must chose an appropriate basis $\{\phi_i, i=1, ..., M\}$ for the approximation of the solution

$$\Psi\approx\Psi^{(M)}=\sum_{i=0}^{M} C_i\phi_i(x,y) \tag{2}$$

with M unknowns C_i.

(b) To determine the unknowns C_i a general matrix eigenvalue problem

$$(\mathbf{H}-\lambda^{(M)}\mathbf{S})\boldsymbol{C}=\mathbf{0} \tag{3}$$

has to be solved. In general, this matrix eigenvalue problem has a very large dimension M.

The theoretical connection between problem (a) and the subproblem (b) is as follows: The Schrödinger equation (1) is coupled to the variational integral

$$J=\int_{\bar{\Omega}}\Psi(\hat{H}\Psi-\lambda\Psi)\,\mathrm{d}\bar{\Omega}=\min\Psi, \tag{4}$$

with λ now the Lagrange multiplier connected to the conservation of the norm of Ψ. Inserting Ansatz (2) into the variational integral J and a variation with respect to the coefficients C_i leads to the equation

$$\sum_{j=0}^{M}(H_{ij}-\lambda^{(M)}S_{ij})C_j=0 \tag{5}$$

with

$$H_{ij}:=\int_{\bar{\Omega}}\phi_i(\hat{H}\phi_j)\,\mathrm{d}\Omega \quad \text{and}$$

$$S_{ij}:=\int_{\bar{\Omega}}\phi_i\phi_j\,\mathrm{d}\Omega\,. \tag{6}$$

Defining matrices $\mathbf{H}=(H_{ij})$ and $\mathbf{S}=(S_{ij})$ we can rewrite (5) as the general eigenvalue problem (3).

For the approximation (2) we use a space discretization of $\bar{\Omega}\subset\mathbb{R}^2$ into 2D triangles and local basis functions defined on these triangles, known as the finite element method (FEM). Our space discretization is an extension of the self-adaptive multilevel finite element discretization of Deuflhard et al. [9] as described below. The subproblems (b) are solved either by a Givens method or by an inverse vector iteration, which takes advantage of the structure of the multilevel FEM. For simplicity we describe the adaptive multilevel FEM discretization first and afterwards the treatment of the subproblems (b).

To apply the FEM to the Schrödinger equation the infinite solution domain $\bar{\Omega}$ must be truncated to a finite volume Ω. Ω is chosen to be sufficiently large so that the solution in $\bar{\Omega}\setminus\Omega$ can be assumed to be zero without affecting the eigenvalue λ. Now Ω is segmented into triangles, leading to a mesh with N_0 grid points. On each triangle the solution Ψ is approximated locally by a number of T polynomial shape functions $\{\varphi_i, i=1, ..., T\}$ (see below) defined only on that triangle:

$$\Psi\approx\sum_{i=0}^{T}c_i\varphi_i(x,y)\quad\text{on a triangle}\,. \tag{7}$$

The local approximations (7) have to be chosen continuously on the transition between adjacent triangles [10]. A set of continuous functions resulting from a combination of the local functions build the basis $\{\phi_i, i=1, ..., M_0, M_0\geqslant N_0\}$ for the zeroth-level approximation (2). Solving the general eigenvalue problem (3) determines approximation $\Psi^{(M_0)}$.

It is obvious that the choice of the grid plays an important role for the quality of approximation (2) and the efficiency of the numerical solutions. Therefore we use a procedure which automatically refines the grid. We start with a very coarse hand made grid, e.g. $N_0=5$ grid points. To improve the approximation we may refine our grid uniformly, e.g. by the standard "red" refinement of each of the triangles into four smaller triangles as illustrated in fig. 1. The number of points in this grid would be increased by a factor of 4. This often used global refinement is very inefficient, because Ω must be very large, whereas the non-trivial part of the solution may be located

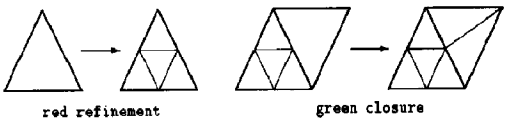

Fig. 1. Refinement of triangles.

only in a certain, small region of Ω. This motivates us to use a self-adaptive local refinement strategy. To decide, which of the triangles have to be selected for an effective grid refinement we need a local error estimator. Therefore the difference between the local approximation (7) and the exact solution on the triangle is approximated for each single triangle, as described in ref. [9]. The error estimator is based on the difference between the solution with linear shape functions and the solution with quadratic shape functions (see below) on the grid (in fact without computing this quadratic solution explicitly). For more details and a rigorous justification we refer to ref. [9]. Now a number of the triangles are selected for refinement according to their contribution to the global discretization error, the so-called basis truncation error. These selected triangles are regular (red) refined and after possible refinement of further triangles, which may be necessary for structural reasons [9,11], the grid is completed by irregular (green) closures as shown in fig. 1. For the refined grid we get a new basis $\{\phi_i, i=1, ..., M_1\}$ with $M_1 > M_0$. Solving the general eigenvalue problem (3) for this basis yields an improved approximation $\Psi^{(M_1)}$. For this approximation $\Psi^{(M_1)}$ we again estimate the local discretization error on each triangle and select the triangles with highest contribution to the basis truncation error for a further refinement. This procedure is repeated level by level, leading to a sequence of approximations (with $M_l > M_{l-1} > ... > M_1 > M_0$), where the grid is automatically adapted to the solution, i.e. becomes more dense in regions where Ψ is most rapidly changing.

The quality of the approximations $\Psi^{(M_l)}$, $l=0, 1, 2, ...$ is not only determined by the sequence of automatically refined grids, but also depends on the form of local shape functions mentioned above. Each shape function φ_i is associated to one of T nodes $\{(x_k, y_k), k=1, ..., T\}$ located on the triangle (as shown in fig. 2) with

$$\varphi_i(x_k, y_k) = \delta_{ik}, \quad k=1, ..., T. \tag{8}$$

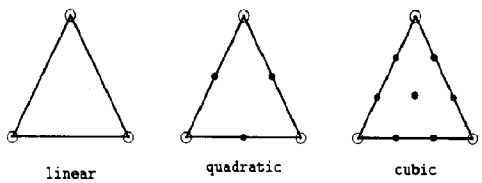

Fig. 2. Position of nodes in a triangle: (⊙) grid point and node; (•) node.

The number of shape functions (and nodes) on each triangle varies with the maximal polynomial order p of the functions, which $\{\varphi_i, k=1, ..., T\}$ can present exactly. Local basis sets for linear ($T=3$), quadratic ($T=6$), and cubic ($T=10$) functions are listed in refs. [12,13]. As a standard linear ($p=1$) functions are used in KASKADE. In addition, we implement shape functions for the polynomial order $p=2$ and 3. The integrals (6) for these functions are computed numerically by an exact or sufficiently accurate Gauss integration formula (see discussion in section 3, below) and the resulting matrices **H**, **S** in (3) are very sparse. Since the matrix dimension corresponds to the number of nodes in the grid (see fig. 2), $p=2$ and $p=3$ induces matrix dimension increases by average factors of 4 and 9, respectively. Moreover, the sparsity of the matrices will be partly destroyed; whereas the average number of non-zeros in a row are 6 for linear shape functions, for $p=2$ and 3 we get 18 and 36 non-zeros, respectively. But in order to achieve higher accuracy it will be necessary to use shape functions of polynomial order 2 or 3 (see section 3).

We now turn to the solution of the subproblem (b), to be solved at each refinement level. For small matrix dimensions (e.g. $M_l \leqslant 50$) the solution of the eigenvalue equation (3) can be computed easily for all eigenvalues by the Givens method [14]. We have to choose one of the eigenvalues $\lambda_i^{M_l}$ (and eigenstate) for the adaptive grid refinement as described above. For higher matrix dimensions the Givens method becomes too costly and we use the inverse vector iteration [14] instead. The inverse vector iteration leads to a sequence of systems of algebraic equations

$$(\mathbf{H} - \gamma \mathbf{S}) C_i = \mathbf{S} C_{i-1}, \quad i=1, 2, 3, 4, ..., \tag{9}$$

where γ is the expected value for the eigenvalue $\lambda_k^{\{M_l\}}$, known from the previous refinement level, i.e. $\gamma = \lambda_k^{\{M_{l-1}\}}$. The initial vector C_0 is choosen as the

corresponding eigenvector on the previous grid (linearly interpolated on the additional grid points). Since $\gamma=\lambda_k^{\{M_{l-1}\}} \approx \lambda_k^{\{M_l\}}$ and $\Psi^{(M_{l-1})} \approx \Psi^{(M_l)}$ the inverse vector iteration (9) converges very fast (less than 3 iterations), especially for dense grids. The resulting eigenvalue is given by

$$\lambda_k^{\{M_l\}}(i)=\frac{\boldsymbol{C}_i^{\mathrm{T}}\mathbf{H}\boldsymbol{C}_i}{\boldsymbol{C}_i^{\mathrm{T}}\mathbf{S}\boldsymbol{C}_i} \tag{10}$$

and the iteration is stopped, when the condition

$$1-\boldsymbol{C}_i^{\mathrm{T}}\mathbf{S}\boldsymbol{C}_{i-1}<10^{-12} \quad \text{for}$$

$$\boldsymbol{C}_i^{\mathrm{T}}\mathbf{S}\boldsymbol{C}_i=\boldsymbol{C}_{i-1}^{\mathrm{T}}\mathbf{S}\boldsymbol{C}_{i-1}=1 \tag{11}$$

is achieved. The solution of the linear systems (9) is computed via an LU-decomposition of the matrix $(\mathbf{H}-\gamma\mathbf{S})$, which takes advantage of the sparsity of the matrix. To minimize the matrix fill-in produced by the LU-decomposition, the numbering of the nodes (basis functions) is reordered by the reverse Cuthill–McKee method [15].

3. Numerical results

For the vibrational motion of a mass in a two-dimensional harmonic oscillator potential we use the Hamilton operator (all quantities in the following are in atomic units)

$$\hat{H}=-\tfrac{1}{2}\nabla^2+k_x x^2+k_y y^2 \tag{12}$$

in $L^2(\mathbb{R}^2, \mathrm{d}^2x)$. The force constants ($k_x=0.5$, $k_y=0.72$) are set according to ref. [16]. We compute the six smallest eigenvalues λ_i, $i=0, 1, ..., 5$ for this problem. For the FEM with linear polynomial shape functions the final results are listed in table 1. Therefore the grids are adaptively refined 10–13 times, leading to general matrix eigenvalue problems with dimension 5 for the initial grid up to dimensions 25000–46000 for the final grids. The final matrix dimension M is restricted by the work space of the workstation being used (Sun SPARC 10). Compared to the FDM results of Alvarez-Collado and Buenker [16] the adaptive refinement strategy leads (for fixed precision) to a reduction of the number of grid points by a factor 3 (λ_0) to 10 (λ_i, $i=1$–5). Moreover the results are variational, i.e. the eigenvalues obtained by the step to step refined grids form strictly decreasing sequences converging from above to the true value (in contrast to the FDM results).

The estimated errors are always in the right range and underestimate the true error by only 30%–40%. Thus, the method enables an error controlled treatment of eigenvalue problems. This is an important advantage, especially in view of a possible extension of the method to molecular electronic structure calculations, where the basis truncation errors (TE) are a major and frequently dominant error source (see, for example refs. [17,18]). In a "log–log" plot (see fig. 3 for the ground state, linear case) the exact error, versus the matrix dimension M can be approximated by a straight line with slope -1. Thus the asymptotic convergence of the adaptive FEM with linear elements is well described by

$$\delta\lambda_i^{\{M\}}:=\lambda_i^{\{M\}}-\lambda_{i,\mathrm{exact}}=\frac{C_i}{M}. \tag{13}$$

This can be used for an extrapolation, e.g. if we use eigenvalues resulting from two refinement levels by the formula

$$\lambda_{i,\mathrm{extr}}=\lambda_i^{\{M_l\}}-(\lambda_i^{\{M_{l-1}\}}-\lambda_i^{\{M_l\}})\frac{M_{l-1}}{M_l-M_{l-1}}. \tag{14}$$

The extrapolated values are also included in table 1. They no longer form upper bounds, but are one digit more accurate and thus may at least be used for a very reliable error estimation.

The increase of the matrix dimension M, to reach higher precision, is restricted by the demand on the CPU and the work space of the computer being used. The matrices are very sparse, but by the LU-decomposition in connection with a reverse Cuthill–McKee reordering, we get an additional matrix fill-in proportional to $M\log M$ [15]. Thus, in our implementation the computational cost grows approximately with $M\log M$. By using an iterative solver instead, for example a conjugate gradient (CG) solver, we may reach at best, a cost which is linear with M. Since for the FEM with linear elements the projection error drops down linearly with M, a desirable precision of 10^{-6} is reachable only with $M\approx 3\times 10^7$. A better way to reach higher-precision results would be to improve the linear convergence behaviour of the method. It is well known that under certain conditions this is possible by higher-order polynomial elements. On the other side the fill-in of the matrices

Table 1
Final results for the FEM with linear polynomial shape functions for the two-dimensional harmonic oscillator (12)

	M [a]	Eigenvalue this work	True error	Estimated error	Eigenvalue eq. (14)	FDM [b]	Exact
λ_0	46357	1.100062	0.62×10^{-3}	0.42×10^{-3}	1.099999	1.0987	1.1
λ_1	34913	2.100232	2.32×10^{-3}	1.65×10^{-3}	2.100039	2.0896	2.1
λ_2	25361	2.300367	3.67×10^{-3}	2.58×10^{-3}	2.300085	2.2911	2.3
λ_3	32087	3.100575	5.75×10^{-3}	3.93×10^{-3}	3.100086	3.0853	3.1
λ_4	26655	3.300811	8.11×10^{-3}	5.85×10^{-3}	3.300091	3.2673	3.3
λ_5	46271	3.500428	4.28×10^{-3}	2.91×10^{-3}	3.499902	3.4829	3.5

[a] M denotes the matrix dimension.
[b] 10201 point grid FDM results of ref. [16].

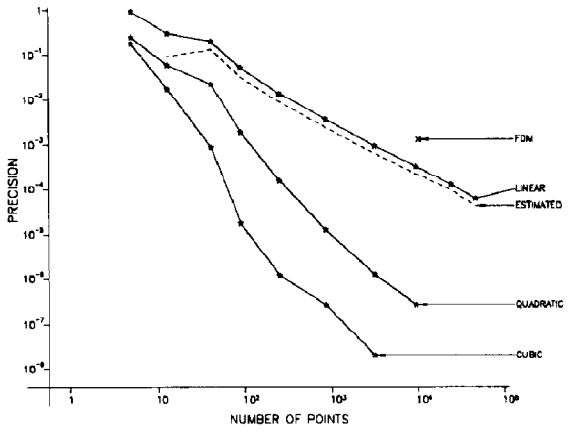

Fig. 3. True and estimated errors for the adaptive FEM treatment of the two-dimensional harmonic oscillator (eq. (12)) at different refinement levels. Also indicated the FDM results of ref. [16].

increases (see section 2) and the method has to face numerical instabilities for very high polynomial orders p. These instabilities result from the numerical integration and the cancellation of high value terms to small numbers. A combination of adaptive grid refinement and moderate p values ($p=1, 2, 3$) seems to be a practicle way to reach precisions in the range 10^{-6}–10^{-8}.

To test the role of the trial function order p we increase p for λ_0 from $p=1$ to $p=2$ (quadratic) for the refinement levels 1–8 and to $p=3$ (cubic) for the levels 1–7. The results are listed in table 2. Whereas the final precision with linear functions is around 6×10^{-5}, with quadratic and cubic functions we get the precision 3×10^{-7} and 2×10^{-8}, respectively. The precision versus number of grid points N for linear, quadratic and cubic functions in the "log–log" of fig. 3 form approximately straight lines with slopes -1, -2, and -3. (The increasing deviation from straight lines for $p>1$ is probably a consequence of the refinement strategy, which was developed for linear local trial functions.) Such a convergence behaviour has favourable implications for the adaptive FEM method. The efficiency of the FEM is determined by the regularity (smoothness in a special sense [13,19]) of the solution and by the polynomial order p of the trial functions to make use of this regularity. The eigenfunction seems to have sufficient smoothness (regularity) that we can estimate the $\delta\lambda$ *by* $|\lambda-\lambda_h|<Ch^{2p}$ (see remark 11.2.21 in ref. [19]), where h is the typical step size of the grid and C a h-independent constant. Since for two-dimensional grids the stepsize h is proportional to $1/N_{\text{grid}}^{1/2}$, a convergence behaviour

$$\delta\lambda_i^{(p)} \sim N_{\text{grid}}^{-p} \tag{15}$$

can be reached by adequately refined grids. A similar behaviour ($\sim N_{\text{grid}}^{-2p}$) was observed by Gázquez and Silverstone [20] for the (one-dimensional) piecewise polynomial approximation of the electronic wavefunction of the helium atom. We get similar efficiency and precision for other (near harmonic) potentials. But it is of greater interest at this point to test the method for the Schrödinger equation of the electron motion in Coulomb potentials, which have singularities.

Therefore we will use the Hamilton operator

$$\hat{H}=-\tfrac{1}{2}\nabla^2+V(x,y,z) \tag{16}$$

Table 2
FEM results for the two-dimensional harmonic oscillator (eq. (12)) at different refinement levels l and for polynomial degree $p=1, 2, 3$

l	M_l	Linear	M_l	Quadratic	M_l	Cubic
1	5	2.051527	13	1.34509524	25	1.27783201
2	13	1.396165	41	1.15940405	85	1.11740377
3	41	1.299124	145	1.12252375	313	1.10088200
4	89	1.152396	337	1.10191236	745	1.10001812
5	249	1.113915	977	1.10015324	2185	1.10000119
6	849	1.103668	3377	1.10001289	7585	1.10000027
7	3125	1.100954	12473	1.10000125	28045	1.10000002
8	9425	1.100326	37669	1.10000027		
9	24013	1.100128				
10	46357	1.100062				
ref. [8]	10200	1.0987				
	exact	1.1				

in $L^2(\mathbb{R}^3, \mathrm{d}^3x)$.

For cylindric-symmetrical potentials V (with $[\hat{l}_z, V]=0$)

$$[\hat{l}_z, \hat{H}]=0 \tag{17}$$

follows. In this case, a change of variables $(x, y, z)\rightarrow(\rho, \varphi, z)$ with cylindrical coordinates

$$\rho=(x^2+y^2)^{1/2}, \quad \varphi=\arctan(y/x) \tag{18}$$

induces the direct sum decomposition

$$L^2(\mathbb{R}^3, \mathrm{d}^3x)=\bigoplus_{m=-\infty}^{\infty} L_m,$$

$$L_m=L^2(\Omega, \mathrm{d}\omega)\otimes \mathrm{e}^{\mathrm{i}m\varphi} \tag{19}$$

with

$$\Omega=\{(\rho, z)\,|\,0<\rho<\infty, -\infty<z<\infty\},$$

$$\mathrm{d}\omega=\rho\,\mathrm{d}z\,\mathrm{d}\rho. \tag{20}$$

For the wavefunction

$$\Psi(\rho, z, \varphi)=\tilde{\Psi}(\rho, z)\mathrm{e}^{\mathrm{i}m\varphi} \tag{21}$$

we get the eigenvalue equation

$$\left[-\frac{1}{2}\left(\frac{1}{\rho}\frac{\partial}{\partial\rho}\rho\frac{\partial}{\partial\rho}+\frac{\partial^2}{\partial^2 z}\right)+\frac{1}{2\rho^2}m^2+V(\rho, z)\right]$$

$$\times\tilde{\Psi}(\rho, \varphi)=E\tilde{\Psi}(\rho, \varphi). \tag{22}$$

Before proceeding, some comments are appropriate.

The FEM is based on the Rayleigh–Ritz variational method and thus the eigenvalues in the FEM are upper bounds of the true energy [21]. But to get variational results, an exact assembling of the matrices, equivalent to an exact evaluation of the integrals (6) is necessary. For harmonic potentials and cubic trial functions a Gauss integration formula of order 8 guarantees this. In the case of Coulomb potentials, however, no exact Gauss integration formula exists, but since the functions are Riemann integrable, accurate results are obtained for any integration formula in the limit $h\rightarrow 0$. This can clearly be seen by inspection of the FEM results for the H_2^+ molecule of Heinemann et al. [3]. Using special coordinates, fifth-order trial functions and increasing the number of points of their grid, they get a final precision of 10^{-10} for the energy, whereas their results, especially for coarse grids, are nonvariational. This may lead to relevant errors for more complicated systems, e.g. for a three-dimensional FEM. To control this error source we increase the accuracy of the proposed integration formula (at least for the final grid) until the energy has converged to a variational value.

Secondly, the singularities of the Coulomb potential producing wavefunction cusps need special attention. Due to those cusps the wavefunction has no arbitrary regularity ($\tilde{\Psi}$ is not in the Sobolev space $H^3(\mathbb{R}^2)\subset C^1(\mathbb{R}^2)$ [19]). On the other hand, Heinemann et al. observed a $1/N_{\mathrm{grid}}^5$ convergence in their results, indicating a high regularity of $\tilde{\Psi}$ away from these cusps. To ensure the convergence of our method and a correct description of these cusps, we auto-

matically refine the triangles containing a Coulomb singularity until the energy has converged. This strategy is also advantageous to avoid accuracy problems of the integration formula at these points.

We now show our method for the solution to the H_2^+ molecule ion by setting

$$V(\rho, z) = -Z_1/[\rho^2+(z-\tfrac{1}{2}R)^2]^{1/2} - Z_2/[\rho^2+(z+\tfrac{1}{2}R)^2]^{1/2}, \quad (23)$$

with $Z_1=Z_2=1$ and $R=2.0$, from which we get the electronic ground state energies listed in table 3. Compared with exact results (see ref. [22] and references therein) this leads to exact errors 6.70×10^{-5}, 7.90×10^{-8} and 1.13×10^{-8}, respectively. This precision corresponds well with the precision of our results for the harmonic oscillator. A 42 point integration formula [23] is sufficient to get variational results for each refinement level. For H_2^+ other groups [3,24,25] have presented fully numerical approaches with partly superior accuracy. With out method, increased accuracy may be reached by using higher polynomial order ($p \geqslant 4$) trial functions. But since the Schrödinger equation is separable in prolate spheroidal coordinates, and at this accuracy level relativistic as well as non-adiabatic effects should be included, as in refs. [3,1], respectively, this would be more of academic interest. The main point is that this adaptive method is not restricted to separable two-center systems. Consequently we use the potential

$$V(\rho, z) = -Z_1/[\rho^2+(z-R_1)^2]^{1/2} - Z_2/[\rho^2+(z+R_2)^2]^{1/2} - Z_3/(\rho^2+z^2)^{1/2}, \quad (24)$$

with $R_1=R_2=1.0$ and $Z_1=Z_2=Z_3=1.0$ to present a kind of bench mark value for the linear triatomic ionic system H_3^{2+}, for which no accurate results, in the sense of 8 or 10 digit accuracy, exist. We get the lowest energy -2.24252332 with cubic functions and a 5509 point grid, leading to the matrix dimension $M=48820$. In view of our results presented earlier, we assume an error of less then 5×10^{-8} for this value. The corresponding energy -2.24252322 for quadratic functions, a 18233 point grid, and matrix dimension $M=72487$, lies 1×10^{-7} below this value. The energy $-2.24245146\pm7.730\times10^{-5}$ for linear functions is reached with a 55449 point grid. These values may be compared with the best estimated eigenvalue -2.2431 by Conroy [26]. The 5509 point triangulation shown in fig. 4, containing 16273 edges and 10765 triangles, may give a qualitative impression of how the grid is adapted automatically to the form of the wavefunction. The triangles are refined up to 16 times; the ratio of the volume of the biggest to the smallest triangle is 4.0×10^8. With respect to the finite element solution, the quality of the triangulation given by the ratio between the radius of the

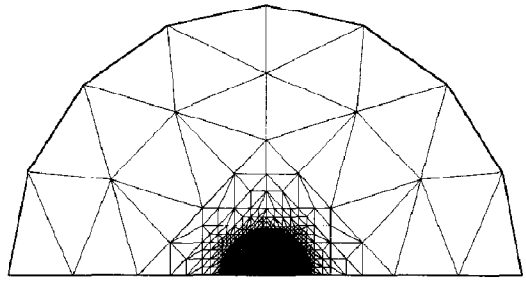

Fig. 4. The adaptive 5509 point grid for the linear H_3^{2+} system, developed from an initial grid with 4 points. The domain is a halfcircle of 19 a_0, whereas the nuclei are located in the middle, 1 a_0 left and right the centre, respectively.

Table 3
Adaptive FEM results for the one-electron systems H_2^+ ($R=2.0$) and linear H_3^{2+} ($R_1=R_2=1.0$)

Shape function	H_2^+			H_3^{2+}	
	M	energy	error	M	energy
linear	25306	-1.10256718	6.70×10^{-5}	55449	-2.24245146
quadratic	37197	-1.10263414	7.90×10^{-8}	72487	-2.24252322
cubic	48970	-1.10263420	1.13×10^{-8}	48820	-2.24252332
exact		-1.10263421			-

inner circle and circumradius, is 0.21 for the worst triangle. A more detailed study of the linear H_3^{2+} would be out of the scope of this Letter.

4. Summary and outlook

We present a new adaptive 2D FEM for the treatment of Schrödinger eigenvalue problems. The method is superior to global basis set expansions and shows several advantages in comparison to standard FEMs applied to quantum-chemical problems:

(i) The method is fully numerical, i.e. is applicable to arbitrary potentials without modifications.

(ii) It is variational and the eigenvalues are true upper bounds for the exact energy.

(iii) The use of a special coordinate system is not necessary and thus, the treatment of problems with more than two Coulomb centers becomes possible.

(iv) The extension to 3D grids is easily possible.

(v) Control over the so-called basis truncation error is given by the error estimator.

This and our results in section 3 show that an adaptive multilevel grid refinement is a very useful too for quantum-chemical calculations. The eigenvalues obtained by the step to step refined grids form strictly decreasing sequences converging from above to the true energy up to a final precision of 8 to 9 significant digits, which is sufficient for most purposes. The estimator for the discretization (or basis truncation) error implemented for linear functions works surprisingly well. But in spite of the fact that the estimated error is always in the right range and leads to grids which are satisfactory also for higher polynomial order trial functions, it would be worthwhile to develop and implement an error estimator for arbitrary polynomial order. Since the polynomial order p and the typical grid size h complement one another to determine the accuracy, our opinion is that this should be done in the form of a h–p method [27]. To make use of the local approximation advantages of the FEM as well as of the high regularity of the solution in wide regions, such a method could offer the possibility to adapt the grid and the polynomial order on each triangle in the most efficient way to a wavefunction. But efforts in this direction would also lead to numerical and implementation problems. Thus, instead of going in this direction, we plan to extend the adaptive method straightforward to 3D grids.

Acknowledgement

We would like to thank our colleagues at the ZIB for helpful comments.

References

[1] J.F. Babb and J. Shertzer, Chem. Phys. Letters 189 (1992) 287.
[2] B. Fricke, D. Heinemann and D. Kolb, Phys. Rev. A 38 (1988) 4994.
[3] D. Heinemann, L. Yang and D. Kolb, Chem. Phys. Letters 178 (1991) 213.
[4] J. Linderberg, Intern. J. Quantum Chem. Symp. Quantum Chem. 19 (1986) 467.
[5] B.H. Wells and S. Wilson, J. Phys. B 22 (1989) 1285.
[6] R. Kornhuber and R. Roitzsch, Commun. Num. Meth. Eng. 9 (1993) 243.
[7] O.C. Zienkiewicz and R.L. Taylor, The finite element method, Vol. 1, 4th Ed. (McGraw-Hill, New York, 1989).
[8] B. Erdmann and R. Roitzsch, KASKADE Manual Technical Report 93-5, Konrad-Zuse-Zentrum, Berlin (1993).
[9] P. Deuflhard, P. Leinen and H. Yserentant, IMPACT Comput. Sci. Eng. 1 (1989) 3.
[10] O. Axelsson and V.A. Barker, Finite element solution of boundary value problems (Academic Press, New York, 1983).
[11] R.E. Bank, PLTMG: A software package for solving elliptic partial differential equations – User's guide 6.0, Frontiers in applied mathematics (SIAM, Philadelphia, 1990).
[12] H.R. Schwarz, Methode der finiten Elemente (Teubner, Stuttgart, 1984).
[13] Ph.G. Ciarlet, The finite element method for elliptic problems (North-Holland, Amsterdam, 1987).
[14] J. Stoer and R. Burlisch, Introduction to numerical analysis (Springer, Berlin, 1980).
[15] A. George and J.W.-H. Liu, Computer solution of large sparse positive definite systems (Prentice-Hall, Englewood Cliffs, NJ, 1981).
[16] J.R. Alvarez-Collado and R.J. Buenker, J. Comput. Chem. 13 (1992) 135.
[17] J. Ackermann and H. Hogreve, Chem. Phys. 157 (1991) 75.
[18] J. Ackermann and H. Hogreve, J. Phys. B 25 (1992) 4069.
[19] W. Hackbusch, Theorie und Numerik elliptischer Differentialgleichungen (Teubner, Stuttgart, 1986).
[20] J.L. Gázquez and H.J. Silverstone, J. Chem. Phys. 67 (1977) 1887.
[21] G. Strang and G.J. Fix, An analysis of the finite element method (Prentice-Hall, Engelwood Cliffs, NJ, 1973).

[22] H. Hogreve, J. Chem. Phys. 98 (1993) 5579.
[23] D.A. Dunavant, Intern. J. Num. Methods Eng. 21 (1985) 1129.
[24] W.K. Ford and F.S. Levin, Phys. Rev. A 29 (1984) 43.
[25] L. Laaksonen, P. Pyykkö and D. Sundholm, Intern. J. Quantum Chem. 23 (1983) 309.
[26] H. Conroy, J. Chem. Phys. 41 (1964) 1327.
[27] W. Gui and I. Babuška, Num. Math. 49 (1986) 613.